

# Development of a New Recycling Process of Shell Wastes Using High-Pressure Carbon Dioxide Solution

Yusuke Kuji<sup>1\*</sup>, Atsushi Iizuka<sup>1</sup>, Yoji Kitajima<sup>2</sup>, Akihiro Yamasaki<sup>3</sup>, and Yukio Yanagisawa<sup>1</sup>

<sup>1</sup>*Department of Environmental Systems, Graduate School of Frontier Sciences, The University of Tokyo*

<sup>2</sup>*Kajima Technical Research Institute, Environmental Engineering and Bioengineering Group, Kajima Corporation*

<sup>3</sup>*Institute for Environmental Management Technology, National Institute of Advanced Industrial Science and Technology (AIST)*

## Abstract

A new recycling process of shell wastes using high-pressure (~ 30 bar) carbon dioxide (CO<sub>2</sub>) solution has been developed. The waste shell composed of the shell part and the flesh part will be crushed and then treated with a high-pressure CO<sub>2</sub> solution. The shell part, mainly composed of calcium carbonate, will be dissolved into the CO<sub>2</sub> solution, and will be separated from the flesh part. The flesh part will be treated in a fermentation process to produce methane gas. The dissolved shell part will be either recovered as calcium carbonate (Process (i)) or will be directly disposed of in the ocean (Process (ii)). Process feasibility was examined with laboratory-scale experimental studies. The dissolution behavior of the blue mussel shell samples with a high-pressure CO<sub>2</sub> solution were investigated under various operation conditions such as the CO<sub>2</sub> pressure, temperature, stirring speed, sample size. The effects of these operation parameters on the shell dissolution rate were elucidated. It was confirmed that the shell sample could be dissolved into high-pressure CO<sub>2</sub> solution with a reasonably high rate, suggesting that the separation of the shell part could be realized by the CO<sub>2</sub> treatment. The methane fermentation experiments demonstrated that the high-pressure CO<sub>2</sub> exposure for 1 hr did not affect the methane fermentation performance of the flesh part of blue mussel. Based on the experimental results, the process design was carried out and the cost was estimated. As a result, the cost of the process (i) (recovery of calcium carbonate) was about 18000 JPY / t-shell, and that of the process (ii) (ocean disposal) was 80,000 JPY /t-shell waste, reflecting the high cost for CO<sub>2</sub> recovery and compression from the flue gas. The process (i) is competitive with the waste disposal cost for simple disposal and more environmentally benign.

## 1. Introduction

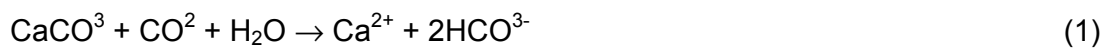
In recent years, disposal of inedible shell wastes, which generate in the inlet and outlet lines of cooling water stream for power plants, have been a serious problem in Japan, where most of large-scale power plants are located in coastal areas <sup>[1]</sup>. The shell wastes consist of shellfish like blue mussels and barnacles adhered on the wall of the water streams. The annual generation rate is as large as 1,500 metric ton per power plant. So far most of the shell wastes have been incinerated or land-filled <sup>[2]</sup>. The incineration treatment is a highly-energy consuming process, and the landfill disposal requires a large disposal site and the rotten shell flesh may emit some bad odor to the

ambient environment. Recycling of the shell waste as a fertilizer has been also examined<sup>[3]</sup> but the demand as a fertilizer has been in a declining trend. Therefore, development of an efficient and environmentally benign treatment process of the inedible shell wastes is needed.

In this paper, we proposed a novel recycling process combining the dissolution and separation process of shell parts with a high-pressure CO<sub>2</sub> treatment with the methane (CH<sub>4</sub>) fermentation process. We examined technical feasibility of the proposed process through laboratory-scale experimental studies under various experimental conditions to optimize operation conditions of the process. Energy and costs for the process were estimated using the obtained experimental results.

## 2. Outline of the proposed processes

The main component of the shell part is calcium carbonate (95 wt%)<sup>[4]</sup> contained in a laminar structure with chitosan, and proteins. The flesh part of seashells consists of mainly organics. The calcium carbonate in the shell part could be used as a calcium source while the flesh part could be used for a fermentation process for energy production. For such a recycling process of the shell waste, it is necessary to separate the shell part and the flesh part from the shell waste, which normally requires a lot of labor. The calcium carbonate component in the shell part could be dissolved in a strong acid while the flesh part is insoluble in acid. Thus it can be anticipated that shell part could be separated from the flesh part with an acid treatment. However, when used a strong acid such as hydrochloric acid, the flesh part could be damaged, and the fermentation performance could be reduced. Instead, high-pressure CO<sub>2</sub> solutions (about 30 bar) were used in this study for the separation of the shell part from the shell wastes. The shell dissolution reaction by carbonic acid can be expressed by the following equation:



The advantages using the high-pressure CO<sub>2</sub> solution are; (1) A significant amount of CO<sub>2</sub> are emitted from the thermal power plant, which is a main target of this process. (2) The damages of the CO<sub>2</sub> treatment on the flesh part could be milder than the case using strong acid because carbonate acid is a weak acid.

There are two options for the treatment of the dissolved calcium carbonate; recovery of the calcium carbonate as high-purity calcium carbonate (Process (i)) and direct discharge of the calcium containing solution into deep sea (Process (ii)). For the former case, the calcium in the aqueous solution can be recovered in the form of CaCO<sub>3</sub> by reducing the CO<sub>2</sub> pressure.



The obtained calcium carbonate could be used for a variety of industrial applications. For the latter case, the CO<sub>2</sub> used for the shell dissolution could be disposed of in the ocean in the form of bicarbonate solution, of which the process can be regarded as a carbon sequestration as a countermeasure for global warming.

The shell flesh part will be remained as a solid phase in the dissolution process, and could be used for the methane fermentation process after the separation. The generated methane can be used for power generation, and the power and the CO<sub>2</sub> generated by the methane combustion could be used in the treatment process of the shell waste.

The process flow diagrams for these two options (Process (i) and Process (ii)) are shown in Figure 1. The high-pressure CO<sub>2</sub> gas used for the shell dissolution process would be supplied from the flue gas of the power plant after capturing and compression. Some part of the CO<sub>2</sub> could be supplied from the combustion process of methane generated from the fermentation process. The shell waste will be crushed in a mill, and then treated in a high-pressure CO<sub>2</sub> solution. Only the shell part of the waste shell will be dissolved in the solution, and separated from the shell waste with filtration or sedimentation. The remained solid phase will be supplied to a methane fermentation reactor, where methane gas will be generated under anaerobic conditions. These operations are common for both options of Process (i) and Process (ii). In the Process (i), the solution phase containing calcium will be transferred to a crystallization process, where the CO<sub>2</sub> pressure was reduced. Due to the reduced solubility of calcium carbonate under lower pressure conditions, calcium carbonate would be precipitated by the pressure reduction. The obtained calcium carbonate could be reused as an industrial material. In the Process (ii), the solution containing calcium ions will be discharged into the deep see, where the pressure is higher than the operation pressure of CO<sub>2</sub> for the dissolution process to avoid the evaporation of gaseous CO<sub>2</sub> from the disposed solution. The process could then be recognized as a sequestration of CO<sub>2</sub>, which can be a countermeasure option for global warming.

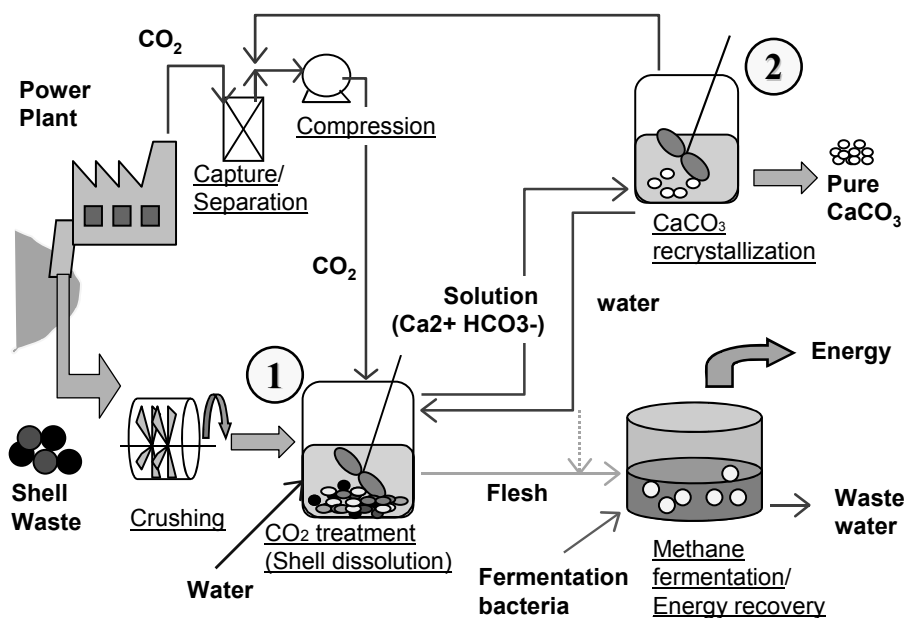


**Figure 1(a).** Flow diagram of the process (i); production of calcium carbonate.

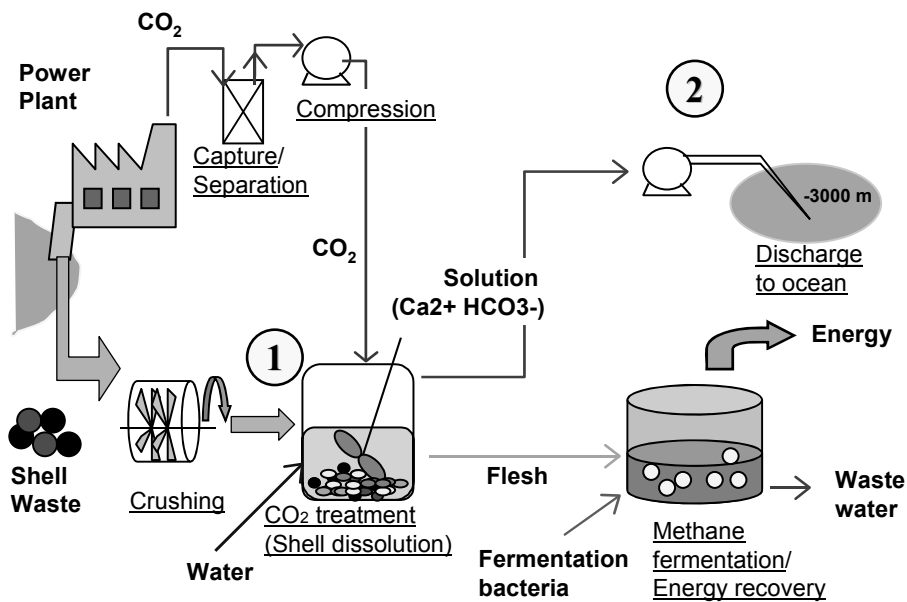


**Figure 1(b).** Flow chart of the process (ii); disposal of carbonate in the ocean.

### 3. High-pressure CO<sub>2</sub> solution treatment

To examine the technical feasibility of the proposed process, laboratory-scale experimental studies were carried out using blue mussels shell samples. In this section the dissolution process of shell part will be discussed.

#### 3.1. Experimental

##### 3.1.1 Shell Waste Sample

Blue mussel shells were used this study. Blue mussel is the dominant species inhabiting the cooling water inlet stream from power plants. After removing the flesh part manually, shell part was crushed and classified by sieving. The mesh sizes of the sieve were 0.30, 0.60, 1.18, and 2.36 mm. The weight fraction of CaCO<sub>3</sub> in the shell was 96 wt%, which was determined by a thermogravimetric technique (Shimazu, DTG-60H)

##### 3.1.2 Experimental apparatus and procedure

Figure 2 shows a schematic diagram of the experimental apparatus. The reactor for the CO<sub>2</sub> treatment was a high-pressure vessel made of a nickel-based alloy, HASTELLOY® with inner volume of 500 mL. The reactor was immersed in a water bath, of which the temperature can be controlled with an accuracy of ± 1 K. The stirring was carried out with two-wing paddle type fins at stirring speed of 0 ~1000 rpm.

A known amount of shell sample (typically 1.0 g) and ion-exchanged water (typically 300 mL) were fed in the reactor under the atmospheric condition. The gas phase was then replaced by CO<sub>2</sub> under a lower pressure condition, and then the CO<sub>2</sub> pressure was increased to a set value for the reaction. The CO<sub>2</sub> was continuously supplied to the reactor from the CO<sub>2</sub> cylinder, and the CO<sub>2</sub>

pressure was kept constant during the experiment by the pressure regulating valve. At a given interval, a small portion (about 1 mL) of the content of the reactor was sampled through the sampling line through a filter (5  $\mu\text{m}$  mesh). The calcium contents in the sampled solution were determined by the inductivity-coupled plasma-atomic emission spectrometry (ICP-AES, Shimadzu, ICPS-7510) to monitor the dissolution rate of calcium from the shell. Effect of the operating conditions such as stirring speed, size of shell sample,  $\text{CO}_2$  pressure, and temperature were investigated on the dissolution behavior of calcium from the shell sample. The experimental conditions were summarized in Table 1.

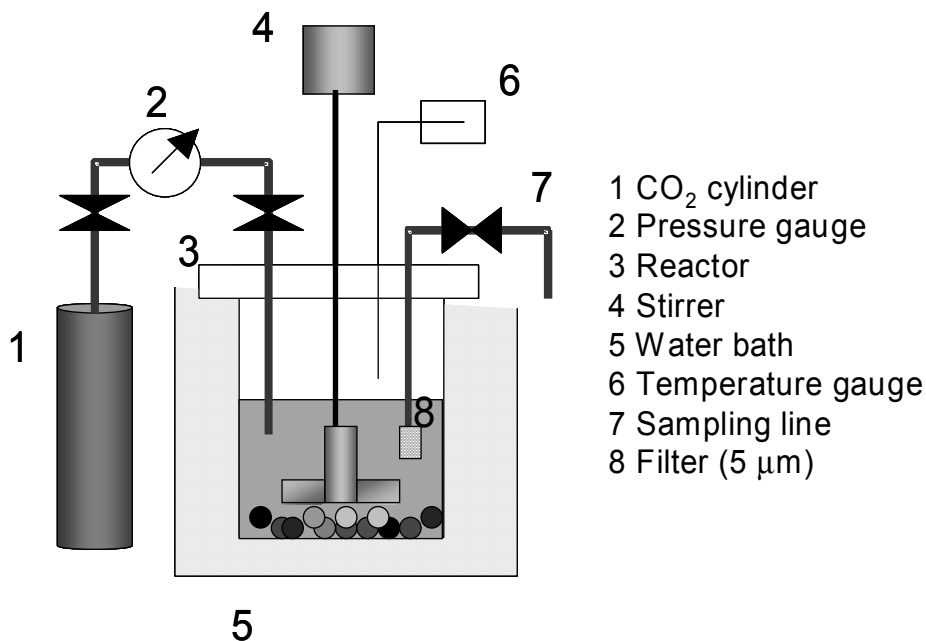


**Figure 2.** Schematic of a high-pressure  $\text{CO}_2$  solution treatment reactor.

**Table 1.** Experimental conditions for high-pressure  $\text{CO}_2$  solution treatment

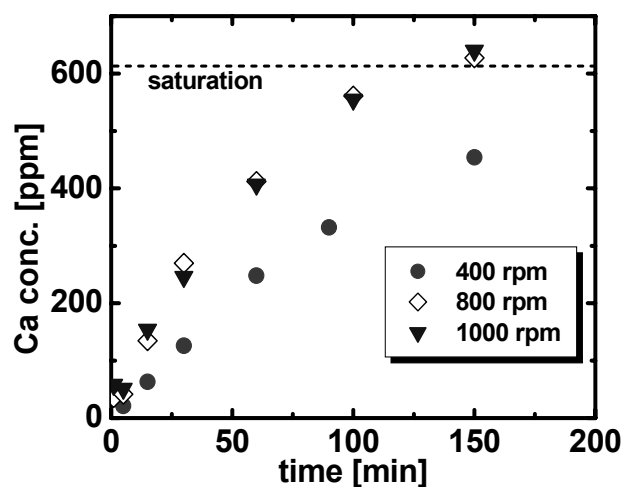
Stirring speed [rpm]	400, 800, 1000
Sample size [mm]	0.30 ~ 0.60, 0.60 ~ 1.18, 1.18 ~ 2.36
$\text{CO}_2$ pressure [bar]	10, 30, 50
Temperature [K]	293, 323, 343

### 3.2. Results and Discussion

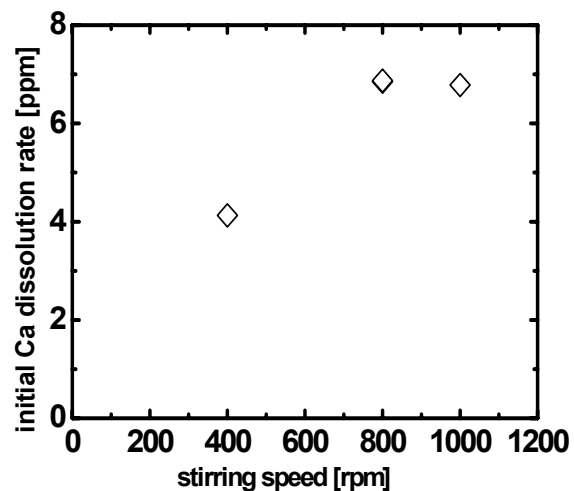
#### 3.2.1. Influence of stirring speed

Figure 3 shows the time variation of the calcium concentration in the solution phase under various stirring speeds. The dotted line in Figure 3 indicates the saturated concentration of calcium ions under the given experimental conditions, which was estimated based on thermodynamic equilibrium. The profile of the calcium concentration change for the stirring speed at 800 rpm was almost equal to the one for the stirring speed at 1000 rpm; the concentration of calcium in the liquid phase increased almost linearly with the reaction time at the initial stage up 60 min, and then

gradually approached the thermodynamic solubility after 150 min of the treatment. On the other hand, when the stirring speed was 400 rpm, the increasing rate of calcium was lower than the cases with higher stirring speed. Figure 4 shows the relationship between the stirring speed and initial dissolution reaction rate of calcium (0 ~ 60 min). The apparent dissolution rate could be explained by a series resistance model of the mass transfer resistance in the liquid phase and the dissolution reaction at the shell surface. These results suggest that the contribution of the mass transfer resistance would become negligible when the stirring speed is greater than 800 rpm. In other words, when the stirring speed is greater than 800 rpm, the apparent dissolution rate is the intrinsic dissolution rate of the shell at the surface. Hereafter, all the dissolution experiments were conducted with a fixed stirring rate at 800 rpm, under the condition the apparent dissolution rate represent the intrinsic reaction rate at the surface without containing the external mass transfer resistance.



**Figure 3.** Influence of the stirring speed on the dissolved calcium concentration in the water phase. shell size: 0.60 ~ 1.18 mm, CO<sub>2</sub> pressure: 30 bar, Temperature: 323 K.

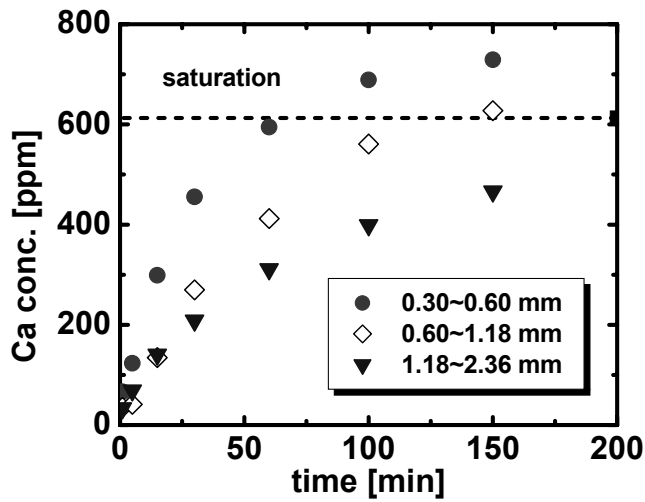


**Figure 4.** Initial rate of the calcium dissolution rate of calcium as a function of the stirring speed.

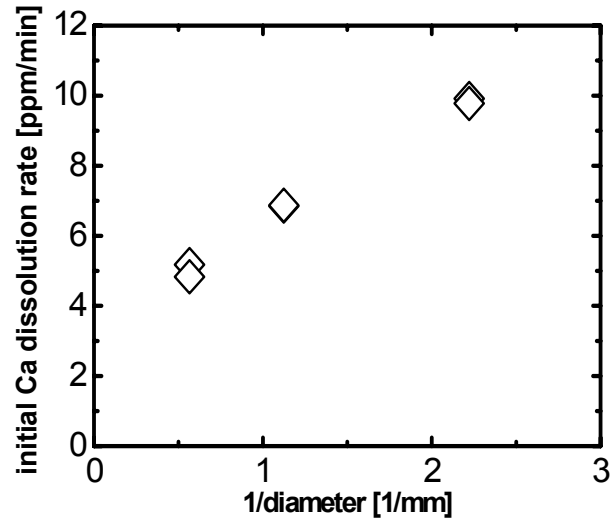
### 3.2.2. Influence of the sample size

Figure 5 shows the time variation of the calcium concentration in the aqueous solution phase during the shell dissolution reaction for various sample sizes. The initial sample weight was equal for all the samples. The dotted line in the figure shows the saturated concentration of calcium under the experimental condition. The smaller shell sample showed higher dissolution rate, and a supersaturation was observed for the case of the sample with the smallest size of 0.30 ~ 0.60 mm. In Figure 6 the initial calcium dissolution rate was plotted against the median diameter of the shell sample, and a linear relation was observed. Under these conditions, the apparent dissolution rate is considered as the (intrinsic) dissolution rate at the surface, and it should be in proportional to the reciprocal diameter of the sample. However, the plot did not pass the origin, although a linear relation was observed. This discrepancy could be explained by the fact that the effective surface area for the dissolution would be different from the spherical case from the following reasons. Shell shape is not

spherical but a plate-like or spicular as shown in Figure 7. Or the calcium contents in the shell could not be extracted uniformly from the surface because of the sandwiched-layered structure of the shell, with the layers of  $\text{CaCO}_3$ , chitosan, and proteins.



**Figure 5.** Influence of the sample size on calcium concentration change in the water phase. Stirring speed: 800 rpm,  $\text{CO}_2$  pressure: 30 bar, Temperature: 323 K



**Figure 6.** The initial calcium dissolution rate of against the reciprocal of the sample size (median diameter).

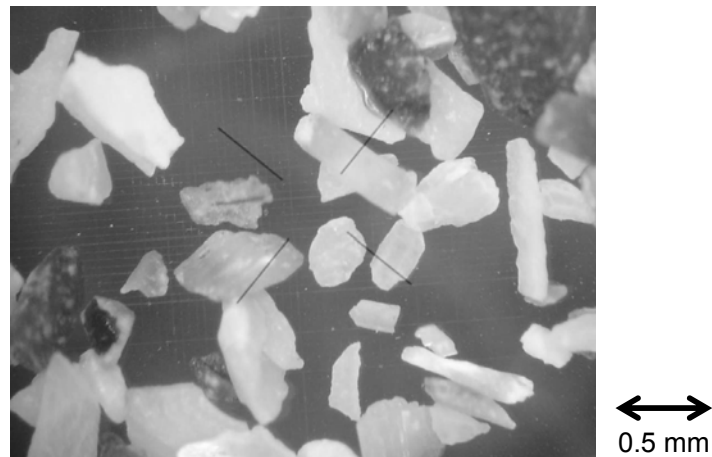
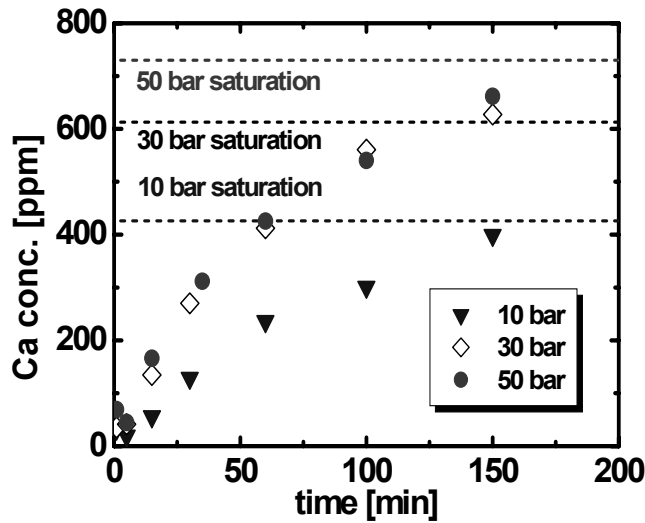


**Figure 7.** Optical microscope image of the crushed shell

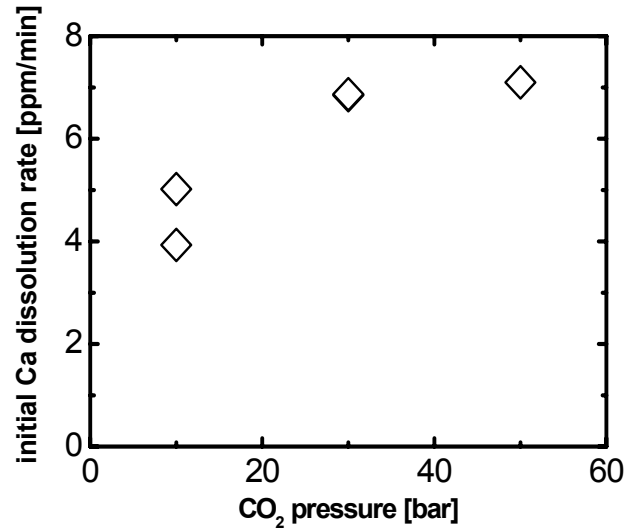
### 3.2.3. Influence of the $\text{CO}_2$ pressure

Figure 8 shows the time variation of the calcium concentration in the solution phase under various  $\text{CO}_2$  pressures. The dotted lines in Figure 8 show the saturated concentrations of calcium in these experimental conditions. The concentration change profile at 50 bar was almost similar for that at 30 bar, while the concentration changing rate was lower at 10 bar. In Figure 9 the initial dissolution rate (0 ~ 60 min) was plotted against the  $\text{CO}_2$  pressure. Because the driving force of the shell dissolution is considered as the difference between the saturation solubility,  $C_{sat}$  and the calcium

concentration in the liquid phase,  $C(t)$ , it is considered that the higher dissolution rate at higher pressure conditions could be due to the higher saturation concentration.



**Figure 8.** Influence of the  $\text{CO}_2$  pressure on calcium concentration change in the water phase. Stirring speed: 800 rpm, sample size: 0.60 ~ 1.18 mm, temperature: 323 K.



**Figure 9.** Initial calcium dissolution rate against the  $\text{CO}_2$  pressure.

### 3.2.4. Influence of the temperature

Figure 10 shows the time variation of the calcium concentration in the solution phase under various experimental temperatures. The dotted lines in the figure show the saturated concentration of calcium under each experimental condition. In Figure 11, the initial calcium dissolution rate for the linear region up to 60 min was plotted against the temperature. The initial dissolution rate showed a maximum at 323 K, although the rate at 343 K was close to that at 323 K. Since the saturation solubility of calcium ions is a decreasing function of the temperature, the observed temperature dependence of the dissolution rate cannot be explained in terms of the driving force,  $C_{sat} - C(t)$ . However, since the kinetic constant for the dissolution reaction,  $k$ , would be an increasing function of the temperature, presumably in an exponential form like the Arrhenius type. Because of these opposite temperature dependences of the driving force and the kinetic constant, the apparent dissolution reaction showed a maximum at an intermediate temperature at 323 K.

From the above experimental studies, it was shown that the shell part of the mussels could be dissolved in the high-pressure  $\text{CO}_2$  solution with a rather high dissolution rate, although the apparent dissolution rates are highly dependent on the dissolution conditions. Therefore, the shell dissolution with high pressure  $\text{CO}_2$  solutions could be applied for the separation of shell and flesh parts of waste shells for recycling.



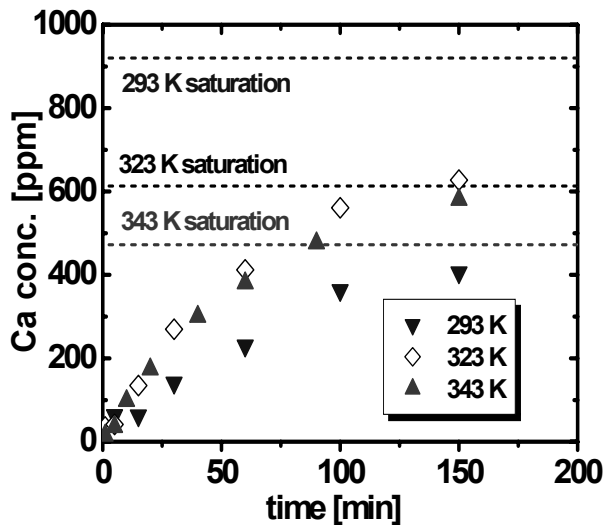


**Figure 10.** Influence of temperature on time courses of calcium concentration in water phase. Stirring speed: 800 rpm, Sample size: 0.60 ~ 1.18 mm, CO<sub>2</sub> pressure: 30 bar

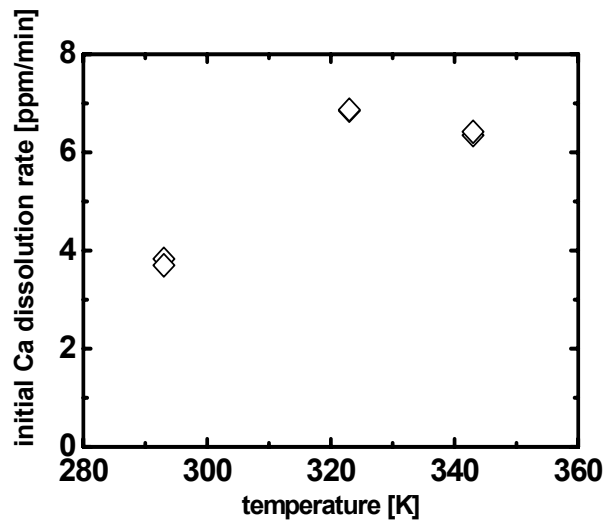


**Figure 11.** Initial calcium dissolution rate of calcium against the temperature.

#### 4. Methane fermentation experiments

In this section, effect of the high-pressure CO<sub>2</sub> treatment on the methane fermentation performances of the shell flesh was examined. This investigation is essential for the possibility of the simultaneous treatment of the flesh part and the shell part with a high-pressure CO<sub>2</sub> for the separation.

##### 4.1. Experimental

###### 4.1.1. Flesh sample

Same type of blue mussel as the dissolution experiments was used in this study. The shell part was manually separated from the mussel sample. The sample flesh was crushed and sieved by a centrifugal filtration. Then 100 mL water was added to the crushed flesh (50 g) to form mince. Total chemical oxygen demand (T-COD) of the flesh mince was about 70,000 ppm.

###### 4.1.2. Experimental apparatus and procedure

0.35 L of the shell flesh mince sample was placed in the high-pressure reactor, and gaseous CO<sub>2</sub> was supplied to the reactor with 30 bar for 1 hr at a stirring speed of 200 rpm and the temperature of 323 K. After the CO<sub>2</sub> exposure, 50 g of the sample flesh was mixed with a methane fermentation liquor of 0.4 L. Then the solution was placed in the methane fermentation incubator at 328 K (EYELA, MTI-202B) (Figure 12). The fermentation was carried out under an anaerobic condition without supplying fresh air. Biogas was collected from a gas sampling line into a gasbag. As a control, fermentation experiments by using flesh sample without a CO<sub>2</sub> exposure was carried out under the same conditions.

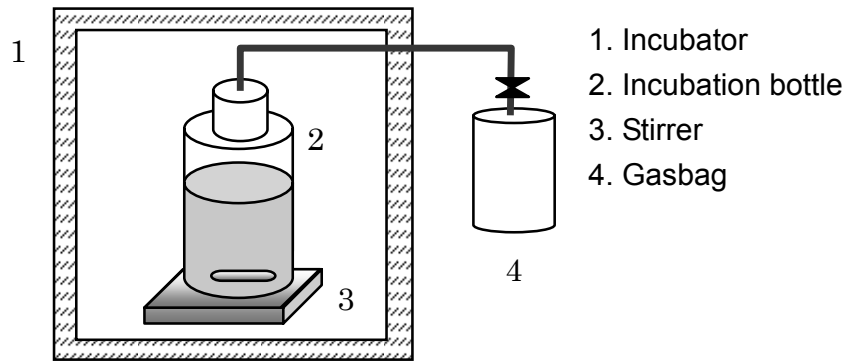


**Figure 12.** Methane fermentation reactor

#### 4.2. Results and Discussion

Figure 13 shows the total biogas generation rate from the flesh samples by the fermentation. It was found that the biogas generation from the flesh sample after a high-pressure CO<sub>2</sub> exposure was almost equal to that from the control flesh sample without the exposure. Figure 14 shows the composition of the generated biogas. No difference was found between the gas compositions between the CO<sub>2</sub>-exposed sample and the control sample. The total methane generation was about 20 mL per 1 g of flesh mince. These results indicate that the methane fermentation performance was unaffected by the high-pressure CO<sub>2</sub> exposure for 1 hr, which is a typical treating time for the shell part dissolution.

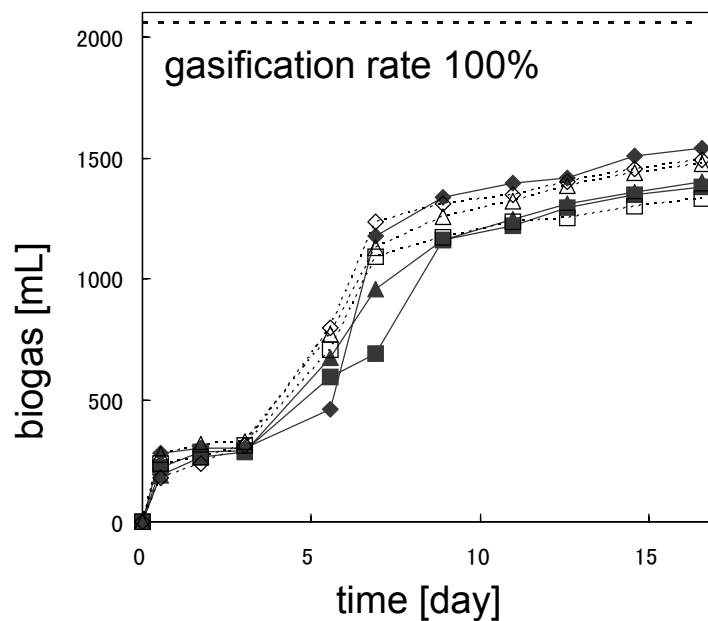


**Figure 13.** Biogas generation rate from the shell samples: Methane fermentation liquor: 0.4 L, Temperature: 328 K. Open keys; CO<sub>2</sub> exposed flesh, closed keys; controlled sample

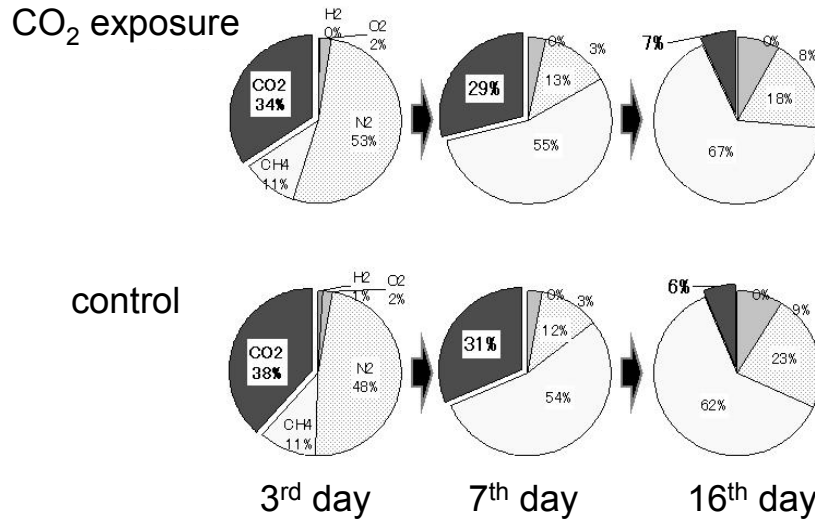


**Figure 14.** Biogas compositions after 3, 7 and 16 days of fermentation.

## 5. Process design and evaluation

From the experimental results, it was shown that the shell part could be dissolved with a high pressure CO<sub>2</sub> exposure, and it was confirmed that the high-pressure CO<sub>2</sub> treatment does not affect the methane fermentation performance of the flesh part. Thus, it was shown the proposed process is technically feasible. In this section, the process design was carried out based on the experimental results and the process cost was estimated.

### 5.1. Process outline and assumptions

Process outline for the two options (Process (i) and Process (ii)) are shown in Figure 1. Both options are comprised of several operations, and cost for each operation was estimated. Operations included common in both Processes (i) and (ii) are, (1) removal of shell waste (2) crushing of the shell waste (3) CO<sub>2</sub> capture and compression from a flue gas stream of a thermal power plant (4) high-pressure CO<sub>2</sub> treatment for the separation of shell part, and (5) methane fermentation of the flesh part. In addition to these ones, (6) crystallization of calcium carbonate will be included in the process (i), and (7) discharge of the dissolved solution into the ocean will be included in the process (ii). For the cost estimation of the processes, costs for the electric power, water supply, CO<sub>2</sub> supply and the plant equipment, along with the revenue by CaCO<sub>3</sub> sales were considered.

In Table 2, the assumptions made for the cost estimation of proposed processes were summarized. The experimentally obtained values in the present study were used for the weight fraction of CaCO<sub>3</sub> in the shell and the calcium dissolution rates were used. Other assumptions were taken from hearing from related companies or literatures.

**Table 2.** Assumptions for the process design

Generation rate of shell waste	1500 t/year/plant
Facilities running	300 days/year
Facilities running	8 h/day
Depletion	15 years
Electrical power expense	2.78 JPY/MJ
Water expense	60 JPY/m <sup>3</sup>
Shell /Flesh (weight ratio)	1
Weight fraction of CaCO <sub>3</sub> (shell)	0.96
Weight fraction of CaCO <sub>3</sub> (flesh)	0
Ca dissolution rate	4 ppm/min

### 5.3. Estimation results

Tables 3, 4 show the estimated cost for each operation in the process (i) and (ii), respectively. The costs shown are per 1 metric ton of the shell waste. Figure 15 shows the total cost of the processes (i) and (ii). The total cost for process (i) was about 18,000 JPY/ t -shell (USD 150) waste, and that of process (ii) was about 80,000 JPY/ t -shell waste (USD 670), which is much higher than that of process (i). The higher cost for the process (ii) is because the high-cost CO<sub>2</sub> after capture and compression cannot be recycled and reused in the process (ii). The cost for the process (i) is comparable with the disposing cost of industrial wastes (just disposal of in a site) in Japan, which is in the range of 15,000 ~ 50,000 (USD 155 ~ 420) JPY / ton-waste. However, the disposing cost is not included the treatment process, but a merely simple disposal in a site. Thus, the present process will be proposed process (i) would be more environmentally benign with a relatively high economical feasibility. On the process (ii) seems disadvantageous due to the high cost of CO<sub>2</sub>. However, the gap could be partially filled by introducing the carbon tax for the CO<sub>2</sub> emission.

**Table 3.** Cost estimation results for the process (i) per 1 ton of the shell.

Process	Removal	Crush	CO <sub>2</sub> Recover	CO <sub>2</sub> Compress	CO <sub>2</sub> Treatment	CaCO <sub>3</sub> Recrystallization	Methane fermentation
Electric power	0	120	0	420	2	2	unkown
Water	0	30	-	-	0	0	-
CO <sub>2</sub>	-	-	4,470	-	-	-	-
Equipment	0	89	0	84	56	56	3,724
Revenue by CaCO <sub>3</sub> sales	-	-	-	-	-	2,400	-

**Table 4.** Cost estimation results for the process (ii) per 1 ton of the shell.

Process	Removal	Crush	CO <sub>2</sub> Recover	CO <sub>2</sub> Compress	CO <sub>2</sub> Treatment	Discharge of ocean	Methane fermentation
Electric power	0	120	0	420	2	500	unknown
Water	0	30	-	-	18,000	0	-
CO <sub>2</sub>	-	-	51,000	-	-	-	-
Equipment	0	89	0	84	56	84	3,724
Revenue by CaCO <sub>3</sub> sales	-	-	-	-	-	-	-

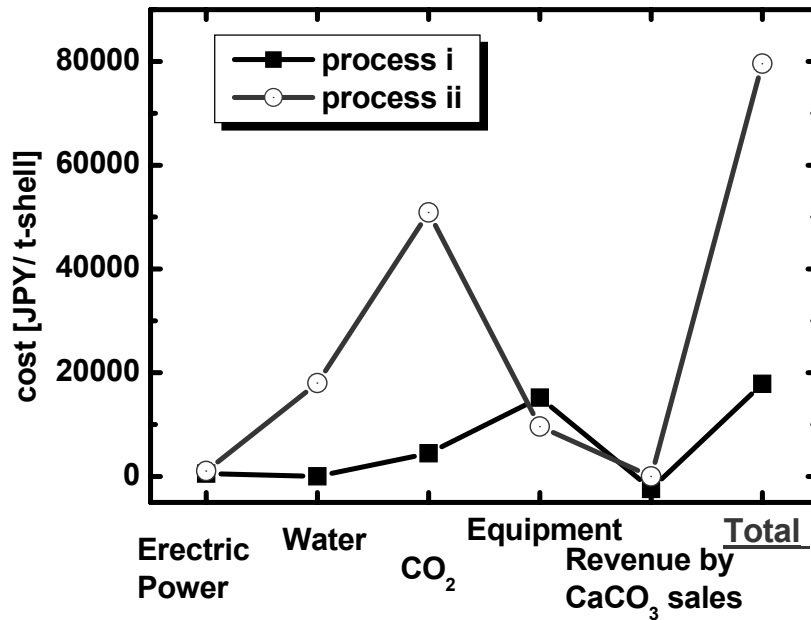


Figure 15. Total Cost of the proposed process

## 6. Conclusions

A new type of recycling process of shell waste was proposed. The shell part could be dissolved using a high-pressure CO<sub>2</sub> solution indicating the shell part and the flesh part can be separated by this operation, and effects of various operation parameters on the dissolution rates of the shell were experimentally studied. The high-pressure CO<sub>2</sub> exposure to the flesh has no noticeable effect on the methane fermentation performance. Therefore, it was confirmed that the proposed process (i) would be technically feasible. The cost for the recycling process of the shell waste was estimated about 18,000 JPY/t-shell waste for the case with calcium carbonate recovery, of which the cost is competitive with that for a simple waste disposal.

## Acknowledgment

This study was financially supported by bounty of KEIRIN under a research study program of Engineering Advancement Association of Japan, and carried out by Kajima Corporation in cooperation with The University of Tokyo.

## References

- [1] T. Yasue, et al.; Journal of the Society of Inorganic Materials. Japan, Vol.8, pp. 58-68, 2001.
- [2] A. Kawabe, et al.; Karyokuhatsuden (Japanese), Vol.54, 230-255.
- [3] S. Imai, et al.; Denryokudoboku (Japanese), Vol.284, pp.1-4, 1999.
- [4] G. L. Yoon, et al.; Waste Management, Vol.23, pp. 825-834, 2003.